Single Electron Pnicogen Bonded Complexes

ARTICLE *in* THE JOURNAL OF PHYSICAL CHEMISTRY A · JANUARY 2014

Impact Factor: 2.69 · DOI: 10.1021/jp412144r · Source: PubMed

3 AUTHORS:

Ibon Alkorta
Spanish National Research Council
680 PUBLICATIONS **12,430** CITATIONS
SEE PROFILE

José Elguero
Spanish National Research Council
1,502 PUBLICATIONS **22,206** CITATIONS
SEE PROFILE

Mohammad Solimannejad
Arak University
167 PUBLICATIONS **1,589** CITATIONS
SEE PROFILE

THE JOURNAL OF PHYSICAL CHEMISTRY A

Article

pubs.acs.org/JPCA

Single Electron Pnicogen Bonded Complexes

Ibon Alkorta,*[,†] Jose Elguero,[†] and Mohammad Solimannejad[‡]

[†]Instituto de Química Médica (IQM-CSIC), Juan de la Cierva, 3, 28006-Madrid, Spain

[‡]Quantum Chemistry Group, Department of Chemistry, Faculty of Sciences, Arak University, Arak 38156-8-8349, Iran

Supporting Information

ABSTRACT: A theoretical study of the complexes formed by monosubstituted phosphines (XH_2P) and the methyl radical (CH_3) has been carried out by means of MP2 and CCSD(T) computational methods. Two minima configurations have been obtained for each $XH_2P{:}CH_3$ complex. The first one shows small P−C distances and, in general, large interaction energies. It is the most stable one except in the case of the $H_3P{:}CH_3$ complex. The second minimum where the P−C distance is large and resembles a typical weak pnicogen bond interaction shows interaction energies between −9.8 and −3.7 kJ mol^{-1}. A charge transfer from the unpaired electron of the methyl radical to the P−X σ^* orbital is responsible for the interaction in the second minima complexes. The transition state (TS) structures that connect the two minima for each $XH_2P{:}CH_3$ complex have been localized and characterized.

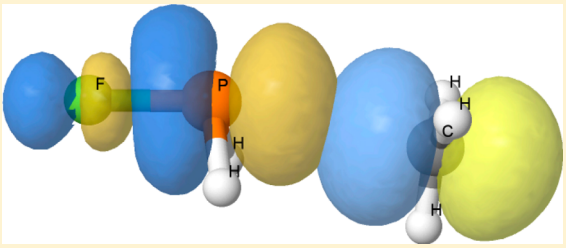

INTRODUCTION

Non-covalent interactions between molecules play a very important role in supramolecular chemistry, molecular biology, and materials science. Although research has traditionally focused on the most common hydrogen bond (HB) interactions, very recently, interest has grown for another type of intermolecular interactions, such as pnicogen bonds.

One of the new HB possibilities corresponds to that where the electron donor is a radical and participates in the HB via a single electron. It has been shown that the unpaired electron of the methyl radical may attract the hydrogen atom of a proton donor, forming a kind of unconventional HB called single electron hydrogen bond.[1−13]

In view of the similarities between halogen bonding and lithium bonding with H-bonding, the existence of a single electron halogen bond[14−17] and a single electron lithium bond[18] has been reported theoretically.

The pnicogen bond has been recognized as a new and important type of intermolecular interaction.[19−48] A pnicogen bond interaction is defined as the one in which the atom of the Lewis acid involved in the interaction is a pnicogen one (N, P, As, or At). It was first noticed when the lone pair of the nitrogen atom of HSN (mercaptoimidogen) interacted with the electron deficient region of PH_3 or other phosphines.[23] Very recently, complexes with pnicogen bonds involving sp^2 hybridized phosphorus atoms have been characterized.[49,50] The nature of the pnicogen bond interaction has been rationalized on the basis of the σ-hole concept.[51] However, a recent report has indicated the possibility to use the Laplacian of the electron density as a predictive tool.[52] To the best of our knowledge, the existence and characterization of a single electron pnicogen bond arising from the interaction of a single electron donor such as methyl radical with phosphines is reported here for the first time even though the homolytic substitution reactions of the hydrogen atom and methyl radical at the phosphorus atom in phosphine and methylphophine have been studied at the MP4 computational level.[53]

Careful studies in simple models are of interest in order to extend their conclusions to more extensive ones. In this article, the methyl radical as a single electron donor molecule and monosubstituted phosphines as electron acceptors have been considered. The methyl radical is a metastable colorless gas and a strong reductant that has been observed in an interstellar medium, while phosphine is known to be a scavenger of methyl radicals.[54] The potential pnicogen bonded complexes between monosubstituted phosphines and methyl radical have been studied using MP2 and CCSD(T) methods. Two minima have been found for each complex. The geometric, energetic, and electronic (spin density, electron density, and natural bond orbital) properties of the minima complexes have been characterized and discussed. In addition, the transition state geometry that connects the two minima has been characterized.

COMPUTATIONAL METHODS

The geometry of the systems has been initially optimized at the UMP2 computational level with the aug′-cc-pvtz basis set. This basis set is composed by the Dunning aug-cc-pVTZ basis[55,56] for the heavy atoms and the cc-pVTZ for H ones. Frequencies were computed to identify equilibrium and transition structures. The UMP2 calculations were performed using the Gaussian 09 program.[57] A further geometry optimization at the UCCSD(T)/aug′-cc-pVTZ level[58,59] has been carried out with the MOLPRO program.[60]

Received: December 11, 2013
Revised: January 14, 2014
Published: January 16, 2014

   dx.doi.org/10.1021/jp412144r | J. Phys. Chem. A 2014, 118, 947−953

The interaction energy of the complexes has been calculated as the difference between the electronic energy of the dimer minus the sum of the isolated monomers in their minima configuration.

The localized molecular orbital energy decomposition analysis (LMOEDA) partition method[61] at the MP2 computational level has been used to compute the interaction energy terms using eq 1.

$$E_{int} = E_{elst} + E_{exch\text{-}rep} + E_{pol} + E_{disp} \quad (1)$$

where E_{elst} is the electrostatic term describing the classical Coulomb interaction of the occupied orbitals of one monomer with those of another monomer and $E_{exch\text{-}rep}$ is the repulsive exchange component resulting from the Pauli exclusion principle. E_{pol} and E_{disp} correspond to polarization and dispersion terms, respectively. The polarization term contains all classical induction, exchange-induction, etc., from the second order up to infinity. These calculations have been carried out with the GAMESS program (version 2013-R1).[62]

Several tools have been used to characterize the electron properties of the systems considered in the present article. The molecular electrostatic properties and spin densities of the systems have been calculated with the facilities of the Gaussian 09 program and plotted using the Jmol program.[63] The natural bond orbital (NBO) method[64] has been used to analyze the stabilizing charge-transfer interactions using the NBO-6 program.[65] NBO orbitals have been represented with the Jmol program[63] using the tools developed by Marcel Patek.[66]

The electron density has been analyzed within the atoms in molecules (AIM) methodology with the AIMAll program.[67] The atomic integration has been carried out to obtain the atomic charges. In all cases, it has been confirmed that the integrated Laplacians in the atomic basins have absolute values smaller than 1×10^{-3}. This condition has proven to provide very small errors in the charge of the systems.[68]

RESULTS AND DISCUSSION

Monomers. The electrostatic potential of the methyl radical, CH_3, present two minima over the carbon atom, one above and the other below the molecular plane (Figure 1). The values of the MEP minima are −0.014 au. This value of the MEP minima is very small when compared to an electron donor with lone pairs like NH_3 (−0.098 au), OH_2 (−0.071 au), or PH_3 (−0.030 au).

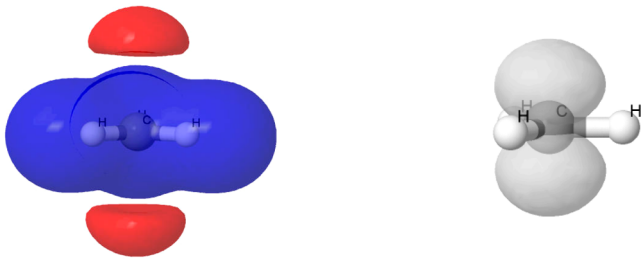

Figure 1. Molecular electrostatic potential and spin density of the methyl radical. The ±0.01 au isosurfaces of the MEP are represented in red (−0.01) and blue (+0.01). The spin density represented corresponds to a value of 0.01.

The representation of the spin density of the methyl radical (Figure 1) shows that it is mainly concentrated in two lobes above and below the molecular plane, centered in the carbon atom.

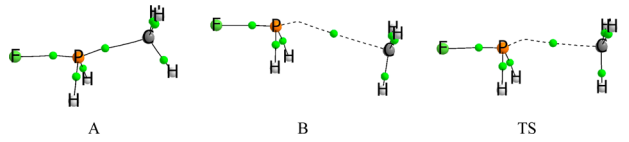

Figure 2. Electron density molecular graphs of the two minima and transition state (TS) found for the $FH_2P{:}CH_3$ complex. The green dots represent the location of the bond critical points of the electron density, and the lines connecting the atoms indicate the bond paths. The geometries and molecular graph of the rest of the systems are gathered in Tables S1−S3 of the Supporting Information.

The electronic properties of the phosphine derivatives have already been discussed[50] and will be only briefly mentioned here. The MEP on the van der Waals surface of the monosubstituted phosphines is characterized by the presence of a minimum and a maximum in the proximity of the phosphorus atom. The minimum is generated by the lone pair of the phosphorus atom, while the maximum is associated with the σ-hole of the P−X bond. In general, as the electronegativity of the X group increases, the value of the MEP in the σ-hole becomes more positive.

$XH_2P{:}CH_3$ Complexes: Energetic and Geometric Aspects. Two minima are found in the potential energy surface that involves the direct interaction of the phosphorus atom of the phosphine and the carbon atom of methyl radical (Figure 2). The first minimum (A) corresponds to short P−C distances, between 1.87 and 1.95 Å, interaction energies that range from −91 to −0.2 kJ mol^{-1} (Table 1). The complexes in this configuration are always more stable than the corresponding ones in configuration B, except for the least stable one $H_3P{:}CH_3$, where the B configuration is more stable. The complexes in configuration A with the shortest and longest P−C distances are the ones with the strongest ($ClH_2P{:}CH_3$) and weakest ($H_3P{:}CH_3$) interaction energies, respectively. In fact, a reasonable linear correlation ($R^2 = 0.94$) can be found between these two parameters in the complexes in configuration A.

The formation of complexes in configuration A has important effects on the geometry of the interacting molecules. Thus, the X−P distances are elongated in all the complexes between 0.22 and 0.07 Å with respect to the corresponding isolated phosphine. In addition, the CH_3 group is clearly pyramidal in the complexes with HCH angles between 108.9 and 110.7° in contrast to the value of 120.0° in the isolated CH_3 molecule.

The second minima, B, present interatomic P···C distances between 3.063 and 3.662 Å and interaction energies between −9.8 and −3.7 kJ mol^{-1} at the MP2 level. The results obtained for these complexes at the CCSD(T) level are very similar to those at the MP2 level. Almost perfect linear relationships are obtained when the interaction energy ($R^2 = 0.996$) or the interatomic P···C distance ($R^2 = 0.999$) at the MP2 and CCSD(T) computational levels are compared.

The interaction energies of the complexes in configuration B are smaller than others described in the literature where the electron donor moiety has a lone pair.[24,25,34,35,69] In fact, the closed shell $XH_2P{:}NH_3$ complexes (see Table S4 of the Supporting Information) present interaction energies that are on average 3 times larger than the corresponding $XH_2P{:}CH_3$ complexes and an intermolecular distance about 0.4 Å shorter in the NH_3 complexes than in the CH_3 ones.

dx.doi.org/10.1021/jp412144r | J. Phys. Chem. A 2014, 118, 947−953

Table 1. Interaction Energy (kJ mol^{-1}), P···C Interatomic Distances (Å) for the Two Minima, and the TSs Calculated at the MP2/aug′-cc-pVTZ and CCSD(T)/aug′-cc-pVTZ, in Parentheses, Computational Levels[a]

	E_i (kJ mol^{-1})			P···C distance		
	A	B	TS	A	B	TS
$FH_2P:CH_3$	−80.9	−9.8 (−10.0)	−7.5	1.886	3.063 (3.058)	2.595
$(NC)H_2P:CH_3$	−52.3	−9.5 (−9.2)	−3.2	1.891	3.146 (3.154)	2.480
$ClH_2P:CH_3$	−91.0	−9.1 (−9.2)	−6.9	1.866	3.098 (3.094)	2.613
$(CN)H_2P:CH_3$	−19.3	−7.1 (−7.4)	8.3	1.916	3.344 (3.342)	2.383
$(OH)H_2P:CH_3$	−60.6	−6.7 (−6.9)	0.1	1.899	3.262 (3.259)	2.539
$(CCH)H_2P:CH_3$	−7.1	−5.4 (−5.6)	13.8	1.942	3.452 (3.441)	2.369
$(CH_3)H_2P:CH_3$	−8.2	−3.8 (−3.9)	16.9	1.942	3.693 (3.676)	2.408
$H_3P:CH_3$	−0.2	−3.7 (−3.7)	19.8	1.947	3.662 (3.658)	2.368

[a]The data have been ordered on the basis of the interaction energy of configuration B.

Table 2. Values of the γ and β Parameters as Defined by eqs 2 and 3

complex	γ	β
$FH_2P:CH_3$	0.94	0.20
$(NC)H_2P:CH_3$	0.77	−0.06
$ClH_2P:CH_3$	0.95	0.21
$(CN)H_2P:CH_3$	0.28	−0.35
$(OH)H_2P:CH_3$	0.80	−0.06
$(CCH)H_2P:CH_3$	0.04	−0.43
$(CH_3)H_2P:CH_3$	0.10	−0.47
$H_3P:CH_3$	−0.08	−0.51

Table 3. LMOEDA Partition Terms (kJ mol^{-1}) of the Complexes in Configuration B

complex	ES	EX-REP	POL	DISP
$FH_2P:CH_3$	−17.9	29.3	−8.5	−13.3
$(NC)H_2P:CH_3$	−15.2	23.6	−6.2	−12.3
$ClH_2P:CH_3$	−17.0	28.5	−7.5	−13.5
$(CN)H_2P:CH_3$	−10.3	17.3	−3.8	−10.1
$(OH)H_2P:CH_3$	−9.9	14.1	−3.4	−8.3
$(CCH)H_2P:CH_3$	−6.7	10.7	−1.9	−7.7
$(CH_3)H_2P:CH_3$	−4.0	7.0	−1.0	−6.2
$H_3P:CH_3$	−4.0	6.7	−1.0	−5.8

The comparison of the interaction energy and the P···C distance in the complexes in configuration B presents an acceptable linear correlation (R^2 = 0.96), as in the case of the complexes in configuration A.

In what respects the geometric changes observed in the monomers due to the complex formation, small modifications are observed when compared to the isolated ones. For instance, the largest variation of the X−P distance is 0.01 Å and the HCH angles in the CH_3 subunit vary between 119.5 and 120.0°.

The structure of the transition state (Figure 2) that connects minima A and B presents P−C intermolecular distances that vary between 2.61 and 2.37 Å. The relative energy of the TSs with respect to the isolated monomers ranges from −7.5 to +19.8 kJ mol^{-1}. The three systems with the strongest complexes in configuration B show negative values of the relative energy, while positive ones are found in the rest.

The geometries of the TS are intermediate between those found in configurations A and B. Thus, the P−X distances are longer than the ones in the isolated phosphine between 0.032 and 0.016 Å and the HCH angles in the CH_3 subunit are between 115.6 and 118.7°.

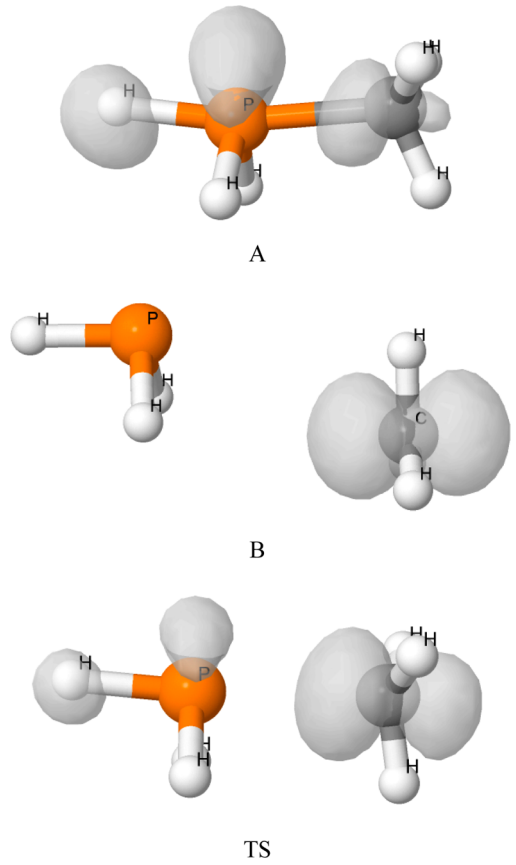

Figure 3. Spin density maps of the $H_3P:CH_3$ minima and TS complexes.

In order to analyze the properties of the TS in relation with the Hammond postulate, two parameters (β and γ proposed by Cioslowski[70]) have been evaluated (Table 2). Equation 2 defines the exothermicity γ as

$$\gamma = \frac{E_B - E_A}{2E_{TS} - E_A - E_B} \quad (2)$$

where E_B, E_A, and E_{TS} are the energies of B, A, and TS, respectively. Equation 3 defines β or the geometrical proximity of the reactants to the transition state

$$\beta = \frac{d(A, TS) - d(B, TS)}{d(A, B)} \quad (3)$$

dx.doi.org/10.1021/jp412144r | J. Phys. Chem. A 2014, 118, 947−953

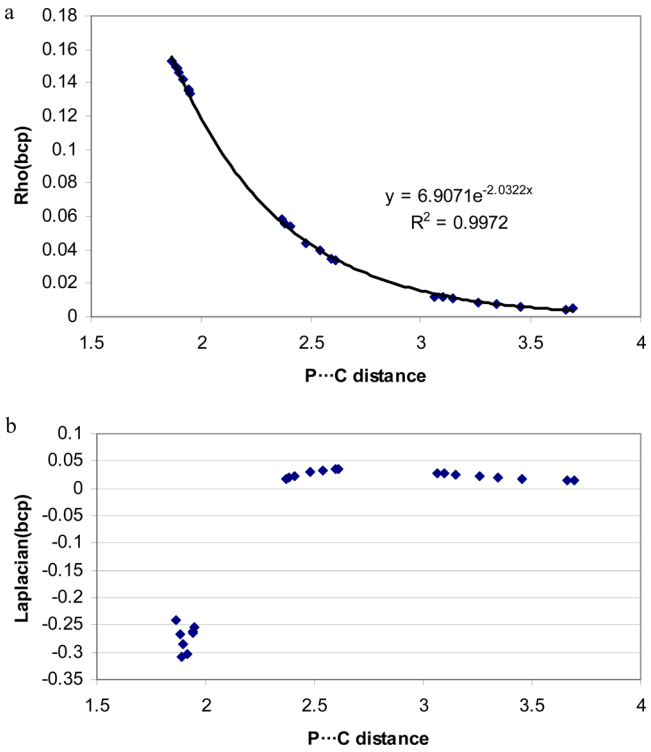

Figure 4. Electron density (a) and Laplacian (au) (b) at the P−C bcp vs the interatomic distance (Å).

Table 4. NBO Stabilization Energy (kJ mol^{-1}) due to the Charge Transfer from the C(lp) toward the P−X σ^* in the $XH_2P{:}CH_3$ Complexes in Configuration B[a]

		charge of CH_3	
	$E(2)$	NBO	AIM
$FH_2P{:}CH_3$	14.77	0.025	0.024
$(CN)H_2P{:}CH_3$	13.43	0.022	0.020
$ClH_2P{:}CH_3$	16.40	0.028	0.021
$(NC)H_2P{:}CH_3$	7.57	0.013	0.013
$(HO)H_2P{:}CH_3$	8.45	0.013	0.014
$(HCC)H_2P{:}CH_3$	5.10	0.008	0.008
$(CH_3)H_2P{:}CH_3$	1.88	0.003	0.001
$H_3P{:}CH_3$	2.68	0.004	0.004

[a]In addition, the total charges (e) of the CH_3 subunit within the complex calculated with the NBO and AIM methods are listed.

where the d values have been evaluated as the absolute value of the difference of the P−C distances. The two parameters defined in eqs 2 and 3 are dimensionless and vary between −1 and +1. Exothermic reactions are characterized by negative values of γ, while endothermic reactions show positive γ values. The β values will be close to 1 when the geometries of B and TS are very similar because then d(B, TS) approaches zero and d(A, TS) approaches d(A, B). Conversely, β will be close to −1 when the geometries of A and TS are alike.

The exothermicity, γ, is positive in all of the cases except in the $H_3P{:}CH_3$ complexes where configuration A is less stable than B. Values as high as 0.94−0.95 for the fluorine and chlorine phosphines are obtained, since the difference in energy of configurations A and B is very large (71 and 82 kJ mol^{-1}, respectively). The β parameter is negative in all cases except in the fluorine and chlorine complexes that present a value of 0.20 and 0.21, respectively. The most negative values of β correspond to the three weakest complexes in configuration B (X = CCH, CH_3, and H) with values of −0.43, −0.47, and −0.51. The negative values of β of these systems indicate that their TSs are more similar to A than to B, while in the case of the halogen derivatives the opposite happens.

In order to gain insight into the contribution of the different terms of the interaction energy in the complexes in configuration B, the LMOEDA methodology has been applied (Table 3). In all of the complexes considered here, the EX-REP term is the larger one in absolute value. Among the three attractive terms (ES, POL, and DISP), the ES one is the dominant one in the strongest complexes, providing up to 46% of the total attractive energy, while in the two weakest complexes its contribution is only 36−37%. The polarization, that corresponds to between 21 and 9% of the total attractive terms, decreases steadily in importance from the strongest complex ($FH_2P{:}CH_3$) to the weakest one ($H_3P{:}CH_3$). Finally, the MP2 dispersion term contributes a 33% of all the attractive terms in the strongest complex and increases its contribution, reaching 55% in the weakest complexes, where it is the most important attractive term.

$XH_2P{:}CH_3$ Complexes: Electronic Aspects. In this section, different electronic aspects of the $XH_2P{:}CH_3$ complexes will be explored. First, the spin density distribution will be considered. In the second part, the electron density will be treated, and in the last part, the NBO results of these complexes will be discussed.

The spin density maps of the complexes in configuration A (Figure 3) show that this property is distributed over the two original molecules, while in the case of the complexes in configuration B it is concentrated only on the methyl radical, resembling the isolated methyl radical (Figure 1). In the case of the TS structures, the spin density is more similar to the one in complexes in configuration B than those in configuration A, but still some spin density remains in the phosphine subunit.

The topological analysis of the electron density of all the complexes, minima and TS, shows the presence of a bcp

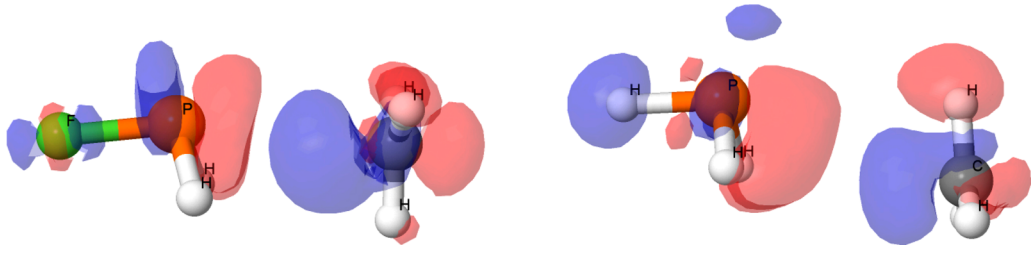

Figure 5. Electron density shift at ±0.0004 au for the $FH_2P{:}CH_3$ complex and ±0.0001 au for the $H_3P{:}CH_3$. Blue and red isosurfaces represent gain and loss of electron density, respectively.

dx.doi.org/10.1021/jp412144r | J. Phys. Chem. A 2014, 118, 947−953

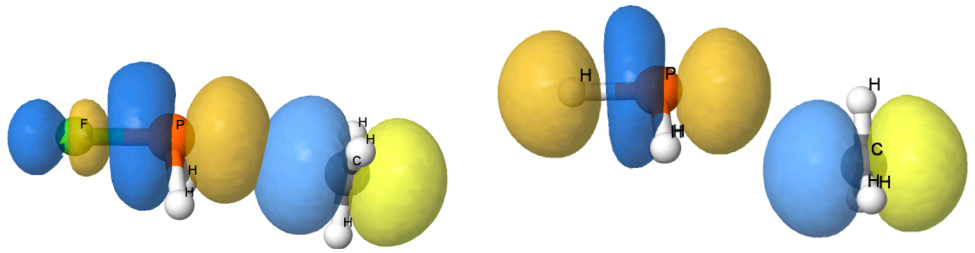

Figure 6. NBO orbitals involved in the stabilizing charge transfer. The C(lp) of the CH_3 molecule and the P−X σ^* orbital in the $FH_2P{:}CH_3$ and $H_3P{:}CH_3$ complexes in configuration B. Positive and negative values of the orbitals are indicated in blue and yellow, respectively.

between the P atom of the phosphine and the C one of the CH_3 subunit. The only exception is the $CH_3H_2P{:}CH_3$ complex (B) that presents a P···H bond path instead of a P···C one. The molecular graphs of the two minima configurations and the TS of the $FH_2P{:}CH_3$ are shown in Figure 2, while those of the rest of the complexes are gathered in the Supporting Information.

The values of the electron density in the bcp are clustered into three groups. Those of the complexes in configuration A present values between 0.153 and 0.134 au which are similar to those found in the covalent P−C bond; for instance, the value of the P−C bcp in the methylphosphine $[(CH_3)H_2P]$ shows a value of 0.152 au. The second group corresponds to the TS structures with values ranging between 0.059 and 0.034 au. Finally, the last group corresponds to the bcp's associated with the complexes in configuration B with values between 0.012 and 0.004 au which are similar to those found in weak interactions but stronger than van der Waals contacts. Using all the P−C bcp data, an excellent exponential relationship between the ρbcp vs the interatomic P−C distance (Figure 4a) is obtained. Similar correlations have been described for pnicogen bonds and other non-covalent interactions.[49,71−75]

The values of the Laplacian at the bcp, as in the case of the electron density, can be clustered into three groups (Figure 4b). Negative values of the Laplacian correspond to those P−C bcp's in the complexes with configuration A. Positive values which increase its value as the interatomic increases too correspond to the TS structures and are associated with the change between the covalent and non-covalent regime of the Laplacian that shows a small maximum in the positive region.[76] Finally, positive values of the Laplacian that decrease as the distance increases are associated with the complexes in configuration B and are typical of weak interactions.

The AIM atomic charges within the complexes show that the CH_3 molecule became positively charged (Table 4). The strongest complexes show a larger positive charge than the weakest ones, with an acceptable linear correlation between the interaction energy and the charge in the CH_3 molecule (R^2 = 0.97).

For a more detailed analysis of the charge transfer due to the complex formation, the electron density shifts of the strongest and weakest complexes in configuration B have been generated (Figure 5). In both cases, a loss of electron density is observed in the face of the CH_3 molecule not involved in the interaction while a gain in the region facing the phosphine molecule. In the proximity of the phosphorus atom, a loss of electron density is observed while a gain is observed at the end of the P−X bond. The effects, even though similar, are 4 times larger in the $FH_2P{:}CH_3$ complex than in the $H_3P{:}CH_3$ one.

The NBO analysis of the intermolecular charge transfer between occupied and empty orbitals shows that the interaction between the unpaired electron of the methyl radical molecule with the σ^* of the P−X bond is the main interaction responsible for the stabilization of the complexes in configuration B (Table 4). The stabilization energy due to this charge transfer ranges between 16.4 and 1.9 kJ mol^{-1}. It should be noted that, even though a rough correlation is found between the interaction energy and the $E(2)$ parameters, in some cases $E(2)$ is larger in absolute value while in others it is smaller, indicating that other factors can modulate these interactions.

A graphical representation of the two orbitals involved in the charge transfer is shown in Figure 6 for the $FH_2P{:}CH_3$ and $H_3P{:}CH_3$ complexes (B). It is clear that in the former complex a larger overlap of the two orbitals involved in the interaction is observed than in the latter complex, in agreement with the different $E(2)$ stabilization energies obtained for these complexes.

CONCLUSION

A theoretical study of the complexes between monosubstituted phosphines and methyl radical has been carried out by means of MP2/aug′-cc-pVTZ and CCSD(T)/aug′-cc-pVTZ computational methods. Two minima have been found in the potential energy surface where the phosphorus of the phosphine interacts with the carbon atom of the methyl molecule. The first one (A) presents short P−C distances and, in general, high interaction energies. The P−C bonds present characteristics similar to those of covalent bonds, and the radical nature of the systems is distributed along the whole system. The second one (B) shows long P−C distances and interaction energies between −9.8 and −3.7 kJ mol^{-1}. In all cases, the A configuration is more stable than the B one, except for the $H_3P{:}CH_3$ complex where the opposite happens. The TS structure connecting the two minima has been characterized for all of the complexes.

The electronic characteristics of the complexes in configuration A are consistent with the formation of a single molecule, while those of B are similar to weak pnicogen bonded complexes. The NBO analysis of the latter complexes indicates that the main stabilization interaction corresponds to a charge transfer from the unpaired electron of the methyl radical toward the σ^* P−X orbital of the phosphine.

ASSOCIATED CONTENT

Supporting Information

Total energy and geometry of the minima and TS of the systems calculated at the MP2/aug′-cc-pVTZ computational level. Interaction energy and intermolecular distance of the analogous $XH_2P{:}NH_3$ complexes. This material is available free of charge via the Internet at http://pubs.acs.org.

AUTHOR INFORMATION

Corresponding Author

*Phone: + 34 91 562 29 00. E-mail: ibon@iqm.csic.es. Web site: http://are.iqm.csic.es.

Notes

The authors declare no competing financial interest.

ACKNOWLEDGMENTS

This work was carried out with financial support from the Ministerio de Economía y Competitividad (Project No. CTQ2012-35513-C02-02) and Comunidad Autónoma de Madrid (Project MADRISOLAR2, ref S2009/PPQ1533). Thanks are also given to CTI (CSIC) for their continued support.

REFERENCES

(1) Chen, Y.; Tschuikow-Roux, E.; Rauk, A. Intermediate Complexes and Transition Structures for the Reactions $CH_3 + HX \rightarrow CH_4 + X$ (X = Cl, Br): Application of G1 Theory. *J. Phys. Chem.* **1991**, *95*, 9832−9836.

(2) Misochko, E. Y.; Benderskii, V. A.; Goldschleger, A. U.; Akimov, A. V.; Shestakov, A. F. Formation of the CH_3-HF Complex in Reaction of Thermal F Atoms with CH_4 in Solid Ar. *J. Am. Chem. Soc.* **1995**, *117*, 11997−11998.

(3) Alkorta, I.; Rozas, I.; Elguero, J. Radicals as Hydrogen Bond Acceptors. *Bunsen-Ges. Phys. Chem., Ber.* **1998**, *102*, 429−435.

(4) Tachikawa, H. A Direct Ab Initio Dynamics Study on the Finite Temperature Effects on the Hyperfine Coupling Constant of a Weakly Bonded Complex. *J. Phys. Chem. A* **1998**, *102*, 7065−7069.

(5) Igarashi, M.; Ishibashi, T.; Tachikawa, H. A Direct Ab Initio Molecular Dynamics Study of the Finite Temperature Effects on the Hyperfine Coupling Constant of Methyl Radical−Water Complexes. *J. Mol. Struct.: THEOCHEM* **2002**, *594*, 61−69.

(6) Alkorta, I.; Elguero, J. Hydrogen Bond Acceptor Properties of Two Radicals: Nitric Oxide Molecule and Hydrogen Atom. *ARKIVOC* **2003**, *xiv*, 31−36.

(7) Wang, B.-Q.; Li, Z.-R.; Wu, D.; Hao, X.-Y.; Li, R.-J.; Sun, C.-C. Single-Electron Hydrogen Bonds in the Methyl Radical Complexes $H_3C\cdots HF$ and $H_3C\cdots HCCH$: An Ab Initio Study. *Chem. Phys. Lett.* **2003**, *375*, 91−95.

(8) Solimannejad, M.; Alikhani, M. E. Theoretical Study of the HCN−CH_3 and HNC−CH_3 Radicals: Hydrogen and Covalent Bonding. *Chem. Phys. Lett.* **2005**, *406*, 351−354.

(9) Solimannejad, M.; Alkorta, I. Competition between Nonclassical Hydrogen-Bonded Acceptor Sites in Complexes of Neutral AH_2 Radicals (A = B, Al, and Ga): A Theoretical Investigation. *J. Phys. Chem. A* **2006**, *110*, 10817−10821.

(10) An, X.; Liu, H.; Li, Q.; Gong, B.; Cheng, J. Influence of Substitution, Hybridization, and Solvent on the Properties of C−HO Single-Electron Hydrogen Bond in CH_3-H_2O Complex. *J. Phys. Chem. A* **2008**, *112*, 5258−5263.

(11) Johnson, E.; Dilabio, G. Radicals as Hydrogen Bond Donors and Acceptors. *Interdiscip. Sci.: Comput. Life Sci.* **2009**, *1*, 133−140.

(12) Li, Q.; Zhu, H.; An, X.; Gong, B.; Cheng, J. Nonadditivity of Methyl Group in Single-Electron Hydrogen Bond of Methyl Radical-Water Complex. *Int. J. Quantum Chem.* **2009**, *109*, 605−611.

(13) Solimannejad, M.; Rezaei, Z.; Esrafili, M. Competition and Interplay between the Lithium Bonding and Hydrogen Bonding: $R_3C\cdots HY\cdots LiY$ and $R_3C\cdots LiY\cdots HY$ Triads as a Working Model (R=H, CH_3; Y=CN, NC). *J. Mol. Model.* **2013**, *19*, 5031−5035.

(14) Li, Q.; Li, R.; Yi, S.; Li, W.; Cheng, J. The Single-Electron Hydrogen, Lithium, and Halogen Bonds with HBe, H_2B, and H_3C Radicals as the Electron Donor: An Ab Initio Study. *Struct. Chem.* **2012**, *23*, 411−416.

(15) Raghavendra, B.; Arunan, E. Unpaired and Σ Bond Electrons as H, Cl, and Li Bond Acceptors: An Anomalous One-Electron Blue-Shifting Chlorine Bond. *J. Phys. Chem. A* **2007**, *111*, 9699−9706.

(16) Li, Z.; Shi, X.; Tang, H.; Zhang, J. Theoretical Study of the Interaction Mechanism of Single-Electron Halogen Bond Complexes $H_3C\cdots Br$-Y (Y = H, CN, NC, CCH, C_2H_3). *Sci. China: Chem.* **2010**, *53*, 216−225.

(17) Solimannejad, M.; Rezaei, Z.; Esrafili, M. Interplay and Competition between the Lithium Bonding and Halogen Bonding: $R_3C\cdots XCN\cdots LiCN$ and $R_3C\cdots LiCN\cdots XCN$ as a Working Model (R=H, CH_3; X=Cl, Br). *Mol. Phys.* **2013**, DOI: 10.1080/00268976.2013.864426.

(18) Li, Y.; Wu, D.; Li, Z.-R.; Chen, W.; Sun, C.-C. Do Single-Electron Lithium Bonds Exist? Prediction and Characterization of the $H_3C\cdots Li-Y$ (Y=H, F, OH, CN, NC, and CCH) Complexes. *J. Chem. Phys.* **2006**, *125*, 084317.

(19) Sundberg, M. R.; Uggla, R.; Viñas, C.; Teixidor, F.; Paavola, S.; Kivekäs, R. Nature of Intramolecular Interactions in Hypercoordinate C-Substituted 1,2-Dicarba-Closo-Dodecaboranes with Short P···P Distances. *Inorg. Chem. Commun.* **2007**, *10*, 713−716.

(20) Tschirschwitz, S.; Lonnecke, P.; Hey-Hawkins, E. Amino-alkylferrocenyldichlorophosphanes: Facile Synthesis of Versatile Chiral Starting Materials. *Dalton Trans.* **2007**, 1377−1382.

(21) Bauer, S.; Tschirschwitz, S.; Lönnecke, P.; Frank, R.; Kirchner, B.; Clarke, M. L.; Hey-Hawkins, E. Enantiomerically Pure Bis-(phosphanyl)carbaborane(12) Compounds. *Eur. J. Inorg. Chem.* **2009**, 2776−2788.

(22) Zahn, S.; Frank, R.; Hey-Hawkins, E.; Kirchner, B. Pnicogen Bonds: a New Molecular Linker? *Chem.—Eur. J.* **2011**, *17*, 6034−6038.

(23) Solimannejad, M.; Gharabaghi, M.; Scheiner, S. SH···N and SH···P Blue-Shifting H-Bonds and N···P Interactions in Complexes Pairing HSN with Amines and Phosphines. *J. Chem. Phys.* **2011**, *134*, 024312.

(24) Scheiner, S. Effects of Multiple Substitution upon the P···N Noncovalent Interaction. *Chem. Phys.* **2011**, *387*, 79−84.

(25) Scheiner, S. Effects of Substituents upon the P···N Noncovalent Interaction: The Limits of Its Strength. *J. Phys. Chem. A* **2011**, *115*, 11202−11209.

(26) Scheiner, S. Can Two Trivalent N Atoms Engage in a Direct N···N Noncovalent Interaction? *Chem. Phys. Lett.* **2011**, *514*, 32−35.

(27) Scheiner, S. On the Properties of X···N Noncovalent Interactions for First-, Second-, and Third-Row X Atoms. *J. Chem. Phys.* **2011**, *134*, 164313.

(28) Scheiner, S. Weak H-Bonds. Comparisons of CHO to NHO in Proteins and PHN to Direct PN Interactions. *Phys. Chem. Chem. Phys.* **2011**, *13*, 13860−13872.

(29) Scheiner, S. A New Noncovalent Force: Comparison of P···N Interaction with Hydrogen and Halogen Bonds. *J. Chem. Phys.* **2011**, *134*, 094315.

(30) Scheiner, S.; Adhikari, U. Abilities of Different Electron Donors (D) to Engage in a P···D Noncovalent Interaction. *J. Phys. Chem. A* **2011**, *115*, 11101−11110.

(31) Li, Q.-Z.; Li, R.; Liu, X.-F.; Li, W.-Z.; Cheng, J.-B. Concerted Interaction between Pnicogen and Halogen Bonds In XCl-FH_2P-NH_3 (X=F, OH, CN, NC, and FCC). *ChemPhysChem* **2012**, *13*, 1205−1212.

(32) Li, Q.-Z.; Li, R.; Liu, X.-F.; Li, W.-Z.; Cheng, J.-B. Pnicogen−Hydride Interaction between FH_2X (X = P and As) and HM (M = ZnH, BeH, MgH, Li, and Na). *J. Phys. Chem. A* **2012**, *116*, 2547−2553.

(33) Blanco, F.; Alkorta, I.; Rozas, I.; Solimannejad, M.; Elguero, J. A Theoretical Study of the Interactions of NF_3 with Neutral Ambidentate Electron Donor and Acceptor Molecules. *Phys. Chem. Chem. Phys.* **2011**, *13*, 674−683.

(34) Del Bene, J. E.; Alkorta, I.; Sanchez-Sanz, G.; Elguero, J. Structures, Energies, Bonding, and NMR Properties of Pnicogen Complexes H_2XP:NXH_2 (X = H, CH_3, NH_2, OH, F, Cl). *J. Phys. Chem. A* **2011**, *115*, 13724−13731.

(35) Del Bene, J. E.; Alkorta, I.; Sanchez-Sanz, G.; Elguero, J. $^{31}P-^{31}P$ Spin−Spin Coupling Constants for Pnicogen Homodimers. *Chem. Phys. Lett.* **2011**, *512*, 184−187.

(36) Alkorta, I.; Sánchez-Sanz, G.; Elguero, J.; Del Bene, J. E. Influence of Hydrogen Bonds on the P···P Pnicogen Bond. *J. Chem. Theory Comput.* **2012**, *8*, 2320−2327.
(37) Del Bene, J. E.; Alkorta, I.; Sanchez-Sanz, G.; Elguero, J. Structures, Binding Energies, and Spin−Spin Coupling Constants of Geometric Isomers of Pnicogen Homodimers $(PHFX)_2$, X = F, Cl, CN, CH_3, NC. *J. Phys. Chem. A* **2012**, *116*, 3056−3060.
(38) Del Bene, J. E.; Alkorta, I.; Sánchez-Sanz, G.; Elguero, J. Interplay of F−H···F Hydrogen Bonds and P···N Pnicogen Bonds. *J. Phys. Chem. A* **2012**, *116*, 9205−9213.
(39) Del Bene, J. E.; Sanchez-Sanz, G.; Alkorta, I.; Elguero, J. Homo- and Heterochiral Dimers $(PHFX)_2$, X= Cl, CN, CH_3, NC: To What Extent Do They Differ? *Chem. Phys. Lett.* **2012**, *538*, 14−18.
(40) Solimannejad, M.; Ramezani, V.; Trujillo, C.; Alkorta, I.; Sánchez-Sanz, G.; Elguero, J. Competition and Interplay Between σ-Hole and π-Hole Interactions: A Computational Study of 1:1 and 1:2 Complexes of Nitryl Halides (O_2NX) with Ammonia. *J. Phys. Chem. A* **2012**, *116*, 5199−5206.
(41) Alkorta, I.; Elguero, J.; Del Bene, J. E. Pnicogen-Bonded Cyclic Trimers $(PH_2X)_3$ with X = F, Cl, OH, NC, CN, CH_3, H, and BH_2. *J. Phys. Chem. A* **2013**, *117*, 4981−4987.
(42) Alkorta, I.; Sánchez-Sanz, G.; Elguero, J.; Del Bene, J. E. Exploring $(NH_2F)_2$, $H_2FP{:}NFH_2$, and $(PH_2F)_2$ Potential Surfaces: Hydrogen Bonds or Pnicogen Bonds? *J. Phys. Chem. A* **2013**, *117*, 183−191.
(43) Del Bene, J. E.; Alkorta, I.; Sánchez-Sanz, G.; Elguero, J. Phosphorus as a Simultaneous Electron-Pair Acceptor in Intermolecular P···N Pnicogen Bonds and Electron-Pair Donor to Lewis Acids. *J. Phys. Chem. A* **2013**, *117*, 3133−3141.
(44) Grabowski, S. J.; Alkorta, I.; Elguero, J. Complexes between Dihydrogen and Amine, Phosphine, and Arsine Derivatives. Hydrogen Bond versus Pnictogen Interaction. *J. Phys. Chem. A* **2013**, *117*, 3243−3251.
(45) Sánchez-Sanz, G.; Alkorta, I.; Trujillo, C.; Elguero, J. Intramolecular Pnicogen Interactions in PHF-$(CH_2)_n$-PHF (n=2−6) Systems. *ChemPhysChem* **2013**, *14*, 1656−1665.
(46) Bauza, A.; Quinonero, D.; Deya, P. M.; Frontera, A. Pnicogen-p Complexes: Theoretical Study and Biological Implications. *Phys. Chem. Chem. Phys.* **2012**, *14*, 14061−14066.
(47) Bauzá, A.; Alkorta, I.; Frontera, A.; Elguero, J. On the Reliability of Pure and Hybrid DFT Methods for the Evaluation of Halogen, Chalcogen, and Pnicogen Bonds Involving Anionic and Neutral Electron Donors. *J. Chem. Theory Comput.* **2013**, *9*, 5201−5210.
(48) Bauza, A.; Quinonero, D.; Deya, P. M.; Frontera, A. Halogen Bonding versus Chalcogen and Pnicogen Bonding: A Combined Cambridge Structural Database and Theoretical Study. *CrystEngComm* **2013**, *15*, 3137−3144.
(49) Alkorta, I.; Elguero, J.; Del Bene, J. E. Pnicogen Bonded Complexes of PO_2X (X = F, Cl) with Nitrogen Bases. *J. Phys. Chem. A* **2013**, *117*, 10497−10503.
(50) Del Bene, J. E.; Alkorta, I.; Elguero, J. Characterizing Complexes with Pnicogen Bonds Involving sp^2 Hybridized Phosphorus Atoms: $(H_2C{=}PX)_2$ with X = F, Cl, OH, CN, NC, CCH, H, CH_3, and BH_2. *J. Phys. Chem. A* **2013**, *117*, 6893−6903.
(51) Politzer, P.; Murray, J. S.; Clark, T. Halogen Bonding and Other s-Hole Interactions: A Perspective. *Phys. Chem. Chem. Phys.* **2013**, *15*, 11178−11189.
(52) Eskandari, K.; Mahmoodabadi, N. Pnicogen Bonds: A Theoretical Study Based on the Laplacian of Electron Density. *J. Phys. Chem. A* **2013**, *117*, 13018−13024.
(53) Schiesser, C.; Wild, L. Homolytic Substitution at Phosphorus: An Ab Initio Study of the Reaction of Hydrogen Atom and Methyl Radical with Phosphine and Methylphosphine. *Aust. J. Chem.* **1995**, *48*, 175−184.
(54) Buchanan, J. W.; Hanrahan, R. J. The Use of Phosphine as a Free Radical Scavenger in the Radiolysis of Methyl Iodide Vapor. *Radiat. Res.* **1970**, *44*, 305−312.
(55) Dunning, T. H. Gaussian-Basis Sets for Use in Correlated Molecular Calculations. 1. The Atoms Boron through Neon and Hydrogen. *J. Chem. Phys.* **1989**, *90*, 1007−1023.
(56) Woon, D. E.; Dunning, T. H. Gaussian Basis Sets for Use in Correlated Molecular Calculations. V. Core-Valence Basis Sets for Boron through Neon. *J. Chem. Phys.* **1995**, *103*, 4572−4585.
(57) Frisch, M. J.; Trucks, G. W.; Schlegel, H. B.; Scuseria, G. E.; Robb, M. A.; Cheeseman, J. R.; Scalmani, G.; Barone, V.; Mennucci, B.; Petersson, G. A.; et al. *Gaussian 09*; Gaussian, Inc.: Wallingford, CT, 2009.
(58) Bartlett, R. J.; Purvis, G. D. Many-Body Perturbation Theory, Coupled-Pair Many-Electron Theory, and the Importance of Quadruple Excitations for the Correlation Problem. *Int. J. Quantum Chem.* **1978**, *14*, 561−581.
(59) Pople, J. A.; Head-Gordon, M.; Raghavachari, K. Quadratic Configuration Interaction. A General Technique for Determining Electron Correlation Energies. *J. Chem. Phys.* **1987**, *87*, 5968−5975.
(60) Werner, H.-J.; Knowles, P. J.; Manby, F. R.; Schütz, M.; Celani, P.; Knizia, G.; Korona, T.; Lindh, R.; Mitrushenkov, A.; Rauhut, G.; et al. *MOLPRO* 2012.1; Cardiff, U.K., 2010.
(61) Su, P.; Li, H. Energy Decomposition Analysis of Covalent Bonds and Intermolecular Interactions. *J. Chem. Phys.* **2009**, *131*, 014102.
(62) Schmidt, M. W.; Baldridge, K. K.; Boatz, J. A.; Elbert, S. T.; Gordon, M. S.; Jensen, J. H.; Koseki, S.; Matsunaga, N.; Nguyen, K. A.; Su, S.; et al. General Atomic and Molecular Electronic Structure System. *J. Comput. Chem.* **1993**, *14*, 1347−1363.
(63) *Jmol: An Open-Source Java Viewer for Chemical Structures in 3D*, version 13.0; http://www.jmol.org/ (accessed Sept 26, 2013).
(64) Reed, A. E.; Curtiss, L. A.; Weinhold, F. Intermolecular Interactions from a Natural Bond Orbital, Donor-Acceptor Viewpoint. *Chem. Rev.* **1988**, *88*, 899−926.
(65) Glendening, E. D.; Badenhoop, J. K.; Reed, A. E.; Carpenter, J. E.; Bohmann, J. A.; Morales, C. M.; Landis, C. R.; Weinhold, F. *NBO-6*; Theoretical Chemistry Institute, University of Wisconsin: Madison, WI, 2013.
(66) Patek, M. *Jmol NBO Visualization Helper*; http://www.marcelpatek.com/nbo/nbo.html (accessed Sept 26, 2013).
(67) Keith, T. A. *TK Gristmill Software*, version 13.11.04; Overland Park, KS, 2013; http://aim.tkgristmill.com (accessed Dec 1, 2013).
(68) Alkorta, I.; Picazo, O. Influence of Protonation on the Properties Derived from Electron Density. *ARKIVOC* **2005**, *ix*, 305−320.
(69) Zahn, S.; Frank, R.; Hey-Hawkins, E.; Kirchner, B. Pnicogen Bonds: A New Molecular Linker? *Chem.—Eur. J.* **2011**, *17*, 6034−6038.
(70) Cioslowski, J. Quantifying the Hammond Postulate: Intramolecular Proton Transfer in Substituted Hydrogen Catecholate Anions. *J. Am. Chem. Soc.* **1991**, *113*, 6756−6760.
(71) Knop, O.; Boyd, R. J.; Choi, S. C. Sulfur-Sulfur Bond Lengths, or Can a Bond Length Be Estimated from a Single Parameter? *J. Am. Chem. Soc.* **1988**, *110*, 7299−7301.
(72) Alkorta, I.; Barrios, L.; Rozas, I.; Elguero, J. Comparison of Models to Correlate Electron Density at the Bond Critical Point and Bond Distance. *J. Mol. Struct.: THEOCHEM* **2000**, *496*, 131−137.
(73) Alkorta, I.; Elguero, J. Fluorine−Fluorine Interactions: NMR and AIM Analysis. *Struct. Chem.* **2004**, *15*, 117−120.
(74) Tang, T. H.; Deretey, E.; Knak Jensen, S. J.; Csizmadia, I. G. Hydrogen Bonds: Relation between Lengths and Electron Densities at Bond Critical Points. *Eur. Phys. J. D* **2006**, *37*, 217−222.
(75) Mata, I.; Alkorta, I.; Molins, E.; Espinosa, E. Universal Features of the Electron Density Distribution in Hydrogen-Bonding Regions: A Comprehensive Study Involving H···X (X=H, C, N, O, F, S, Cl, π) Interactions. *Chem.—Eur. J.* **2010**, *16*, 2442−2452.
(76) Espinosa, E.; Alkorta, I.; Elguero, J.; Molins, E. From Weak to Strong Interactions: A Comprehensive Analysis of the Topological and Energetic Properties of the Electron Density Distribution Involving X−H···F−Y Systems. *J. Chem. Phys.* **2002**, *117*, 5529−5542.